



Published in final edited form as:

*Biochemistry*. 2010 June 22; 49(24): 4998–5006. doi:10.1021/bi100080p.

## Molecular Organization of the Complex Between Muscarinic M3 Receptor and Regulator of G Protein Signaling G $\beta_5$ -RGS7

Simone L. Sandiford, Qiang Wang, Konstantin Levay, Peter Buchwald, and Vladlen Z. Slepak\*

University of Miami Miller School of Medicine, Department of Molecular and Cellular Pharmacology

### Abstract

Regulator of G protein signaling (RGS) complex, G $\beta_5$ -RGS7, can inhibit signal transduction via the M3 muscarinic acetylcholine receptor (M3R). RGS7 consists of three distinct structural entities: the DEP domain and its extension DHEX, the G gamma like (GGL) domain, which is permanently bound to the G protein beta subunit G $\beta_5$ , and the RGS domain responsible for the interaction with G $\alpha$  subunits. Inhibition of the M3R by G $\beta_5$ -RGS7 is independent of the RGS domain but requires binding of the DEP domain to the 3<sup>rd</sup> intracellular loop of the receptor. Recent studies identified the dynamic intramolecular interaction between the G $\beta_5$  and DEP domains, which suggested that the G $\beta_5$ -RGS7 dimer could alternate between the “open” and “closed” conformations. Here, we identified point mutations that diminish DEP:G $\beta_5$  binding, presumably stabilizing the open state, and tested their effects on the interaction of G $\beta_5$ -RGS7 with the M3R. We found that these mutations facilitated binding of G $\beta_5$ -RGS7 to recombinant 3<sup>rd</sup> intracellular loop of M3R, but did not enhance its ability to inhibit M3R-mediated Ca<sup>2+</sup> mobilization. This led us to the idea that the M3R can effectively induce the G $\beta_5$ -RGS7 dimer to open; such a mechanism would require a region of the receptor distinct from the 3<sup>rd</sup> loop. Indeed, we found that the C-terminus of M3R interacts with G $\beta_5$ -RGS7. Truncation of the C-terminus rendered the M3R insensitive to inhibition by the wild-type G $\beta_5$ -RGS7, however, the open mutant of G $\beta_5$ -RGS7 was able to inhibit signaling by the truncated M3R. The GST fusion of M3R C-tail could not bind to wild-type G $\beta_5$ -RGS7 but could associate with its open mutant as well as to the separated recombinant DEP domain or G $\beta_5$ . Taken together, our data are consistent with the following model: interaction of the M3R with G $\beta_5$ -RGS7 causes the DEP domain and G $\beta_5$  to dissociate from each other and bind to the C-tail; the DEP domain also binds to the 3<sup>rd</sup> loop, thereby inhibiting M3R-mediated signaling.

### Keywords

G proteins; RGS proteins; DEP domain; Gbeta5; Muscarinic M3 Receptor

G protein coupled receptors (GPCRs) mediate many physiological processes including neuronal transmission and hormonal regulation. According to the classical model of GPCR signaling, an activated receptor interacts with a heterotrimeric G protein causing the exchange of GDP bound to the G protein  $\alpha$  subunit (G $\alpha$ ) for GTP (1,2). Binding of GTP results in the dissociation of G $\alpha$  from the G $\beta\gamma$  complex (3), and both G $\alpha$ -GTP and G $\beta\gamma$  influence activities of effector enzymes or ion channels (4–6). The return of the GPCR-mediated pathway to its basal state involves hydrolysis of GTP by the G protein. For most G

\*To whom correspondence should be addressed. 1600 NW 10<sup>th</sup> Ave, Miami, FL 33156, USA, Phone: (305)-243-3430, Fax: (305)-243-4555, v.slepak@miami.edu.

proteins, rapid GTP hydrolysis requires participation of regulators of G protein signaling (RGS) proteins, which act as GTPase activating proteins (GAPs) for G $\alpha$  subunits. Over 30 mammalian RGS proteins have been discovered. Outside of the conserved 120 amino acid RGS domain that is responsible for the GAP activity, RGS proteins are very diverse, ranging from ~25 to 120 kDa. According to this diversity, they are classified into distinct subfamilies (reviewed in: (7–11)).

The R7 family of RGS proteins (RGS6, 7, 9 and 11) is defined by the presence of the N-terminal DEP and DHEX domains (Dishevelled, Egl10, Pleckstrin (DEP) and DEP helical extension, respectively), the centrally located GGL domain (G Gamma Like), and the C-terminal RGS domain (12–14). The GGL domain associates permanently with the G protein beta subunit G $\beta_5$  (15–17). The DEP domain binds to R7BP (R7 binding protein), a palmitoylated neuronal protein that can recruit G $\beta_5$ -R7 dimers to the plasma membrane (18–20). Biochemical studies and crystallography showed that the DEP domain and the G $\beta_5$  subunit also bind to each other (21,22).

R7 proteins are implicated in the regulation of neuronal processes such as sensory transduction, locomotor activity and addiction (23). At the molecular level, their function is primarily associated with negative regulation of the Gi family of G proteins. It was shown that R7 proteins do not possess GAP activity for Gq *in vitro* (24). However, in *C. elegans* the R7 protein EAT-16 antagonizes the function of Egl-30, the ortholog of Gq (25–27) and in transfected mammalian cells RGS7 was shown to down-regulate signaling via the Gq-coupled muscarinic M3 receptor, M3R (21,28,29). In a recent report we showed that this regulation occurs via a novel mechanism that does not require GAP activity, but instead involves direct binding of the RGS7 DEP domain to the 3<sup>rd</sup> intracellular loop of the M3R (M3Ri3) (30). In the M3R, this loop is unusually long (more than 200 amino acids) and was previously shown to interact with multiple proteins including Gq (31),  $\beta$ -arrestins (32), G $\beta\gamma$  subunits (33,34), calmodulin (35), and the phosphatase inhibitor SET (36), as well as to contain phosphorylation sites for several kinases (37,38).

In this study we sought to investigate the significance of the DEP:G $\beta_5$  intramolecular interaction in the association of the G $\beta_5$ -RGS7 complex with M3R.

## MATERIALS AND METHODS

### Reagents and Antibodies

Fura 2AM was obtained from Invitrogen. Unless otherwise noted, all chemicals were obtained from Sigma. Rabbit RGS7 (1:1000), G $\beta_5$  (1:1000), and G $\beta_1$  (1:10,000) antibodies have been described earlier (28). Anti-Flag-M2 HRP conjugate was from Sigma (1:5000) and a mouse anti GFP antibody JL-8 was from Clontech (1:1000). Anti-rabbit (1:5000) and anti-mouse (1:3000) secondary antibodies conjugated to peroxidase were from Jackson laboratories. Anti-rabbit fluorescein-labeled antibodies (1:400) were from Amersham Biosciences and anti-mouse Cy3-labeled antibody (1:400) was from Sigma.

### Cell culture, transfection and lysate preparation

CHO-K1 cells were cultured in F-12K Nutrient Mixture (Kaighn's modification) with 10% FBS and penicillin/streptomycin, and plated to the density of  $0.8 \times 10^6$ – $1.0 \times 10^6$  cells per 100 mm plate 24 hours prior to transfection. Transfection was carried out using Lipofectamine (Invitrogen) in accordance with the manufacturer's instructions, as described earlier (28). The ratio of RGS7 to G $\beta_5$  DNA was maintained at 5:1, with a total of 8.0  $\mu$ g of DNA per plate. LacZ DNA was used as a control to ensure that the total DNA per plate remained constant.

After transfection, cells were washed with PBS and lysed in the hypotonic buffer (5 mM Tris-HCL pH 7.6, 0.1 mM MgCl<sub>2</sub>, 1 mM DTT and protease inhibitors cocktail, Roche). Cells were freeze-thawed twice and centrifuged at 14,000 rpm for 45 minutes. The supernatant (total protein concentration 1.0–1.5 mg/ml) represented the cytosolic fraction and was used for the pull-down assays involving cytosolic proteins.

### Cloning of GST fusion proteins

The following GST fusion constructs were generated for bacterial expression and subsequent purification for use in the GST pull-down assay.

**R7-DEP**—Nucleotides 100–372 (corresponding to amino acids 34–124 of bovine RGS7) were PCR amplified from the full-length RGS7 cDNA and cloned into the pGEX-KG vector, as previously described (21). The mutant forms of the GST-DEP constructs were also generated by PCR-mediated mutagenesis utilizing the primers containing the desired substitutions. The RGS7 amino acids were substituted to the corresponding RGS9 residues in the K52S mutant and triple mutants K52S/E73S/D74G and D29A/R33D/K38D. RGS7 residues were substituted with alanine in the F57A mutant and double mutants F49A/L50A and F107A/F110A. All these R7-DEP mutants were cloned into the pGEX-KG vector linearized with BstBI and HindIII.

### The third intracellular loop of the M3 receptor, GST-M3i3

The GST fusion of the third intracellular loop of human muscarinic M3 receptor (amino acids 345–390) was described earlier (30).

### The C termini of Muscarinic receptors

The DNA fragment encoding the M3R C terminus (Asn<sup>548</sup>-Leu<sup>590</sup>) was amplified from the full length human M3R and cloned into the pGEX-2T vector at the BamH1 and EcoR1 sites. The PCR fragments corresponding to the C-terminal amino acid residues of human M1R (Asn<sup>422</sup>-Cys<sup>460</sup>) and M5R (Asn<sup>499</sup>-Pro<sup>532</sup>) were cloned in the same manner.

### Constructs for expression in mammalian cells

**RGS7<sup>249-469</sup>**—This RGS7 construct, described before (21) lacks the DEP and DHEX domains of RGS7 and was generated by PCR amplification of nucleotides 745–1410 (corresponding to amino acids 249–469). The fragment was incorporated into the pcDNA3.0 vector linearized with BamHI and NotI.

**YFP-R7**—RGS7 cDNA was cloned into the pEYFP-C1 vector and has been previously described (29).

**RGS7<sup>ED/SG</sup>**—The double mutation E73S/D74G was introduced into full-length RGS7 using the same primers used for creation of the GST-fusion of the E73S/D74G R7-DEP double mutant (21).

**YFP-R7<sup>F107A/F110A</sup>**—RGS7 cDNA was cloned into the pEYFP-C1 vector at the BglII and HindIII sites. The F107A/F110A double mutation was introduced using the same primers used for the generation of the F107A/F110A R7-DEP mutant.

**YFP-DEP**—Nucleotides 1–372 corresponding to the N terminus and the DEP domain of bovine RGS7, were PCR amplified from full-length RGS7 and cloned into the pEYFP-C1 vector at the BglII and HindIII sites, as previously described (30).

**Gβ<sub>5</sub> mutants**—Gβ<sub>5</sub> cDNA was cloned into the pcDNA3.0 vector at the BamHI and NotI sites. Gβ<sub>5</sub> mutants K54A, R56A/R57A, K60A, H62A, W107A, D259A I282A/I283A and F284A were generated by substituting the named amino acids for alanines using primers containing the mutations. The PCR generated fragments were then cloned into the pcDNA3.0 vector at the BamHI and NotI sites.

The CFP-Gβ<sub>5</sub> construct has been previously described (29,39).

**Truncated M3R (M3R-ΔC)**—The human M3R construct that lacks most of the C terminus was produced by introducing a stop codon at position 565 as previously described (40) and was kindly provided by Dr. Andrew Tobin (University of Leicester).

### GST pull-down assay

The GST pull-down assays were performed as previously described with minor modifications (21,30). Glutathione Sepharose 4B beads were pre-washed with PBS + 0.1% CHAPS and incubated at 4°C with purified GST or the GST fusion proteins for 1–2 hours. Purified GST or a GST fusion protein were immobilized on the matrix at the ratio of 0.15–0.3 μg per μl of packed resin; the amount of immobilized protein was determined by a Bradford protein assay (Pierce) and verified by SDS-PAGE stained by Coomassie. After three washes with PBS + 0.1% CHAPS, the slurry was mixed with the cell lysates required by the experiment and incubated overnight at 4°C on a rotary shaker. At the end of the incubation, the agarose beads were settled by gravity and the supernatant was collected as the unbound fraction. The resin was extensively washed with PBS + 0.1% CHAPS and then eluted with SDS-containing sample buffer. In a typical assay, the packed volume of the resin was 30 μl, and the volume of the protein lysate was 300 μl. The beads were washed three times with 600 μl of PBS + 0.1% CHAPS buffer, and eluted with 30 μl of 2x SDS-PAGE sample loading buffer. The input (total cell lysate), the unbound and eluted fractions were resolved on a 10% SDS gel and analyzed by western blotting. In routine experiments where only 5–20% of the protein subject to the pull-down was captured by the beads (i.e., using the GST fusions of the M3R fragments) and there was no appreciable difference between the total and unbound fractions, we only analyzed the unbound and eluted material.

### Calcium mobilization assay

The cDNA clone for the human muscarinic M3 receptor was obtained from the Missouri S&T cDNA Resource Center ([www.cdna.org](http://www.cdna.org)). CHO-K1 or CHO-R7BP (30) cells were transiently transfected and plated on 12 mm glass coverslips (Electron Microscopy Sciences). After transfection, cells were washed with Hank's Buffered Saline Solution (HBSS) supplemented with 2% FBS in and incubated in the same medium containing 1 μM fura-2AM for 45 minutes at ambient temperature in darkness. The cells were then incubated for 30 min in Locke's buffer (20mM Hepes, 128mM NaCl, 5mM KCl, 1.2mM Na<sub>2</sub>HPO<sub>4</sub>, 2.7mM CaCl<sub>2</sub> and 10mM Glucose) to allow de-esterification of fura-2AM. The coverslips were then secured in a flow chamber and mounted on the stage of a Nikon TE2000 inverted fluorescence microscope. The chamber was continuously perfused with Locke's buffer under gravity flow and cells were stimulated with carbachol solution in the same buffer.

The images were collected using a 20x UV objective lens every two seconds using Metafluor software. The excitation wavelengths were 340 and 380 nm and the emission was set at 510 nm. Free Ca<sup>2+</sup> concentration was determined from the fluorescence measurements on the basis of calibration performed with the fura-2 Ca<sup>2+</sup> imaging kit (Molecular Probes) according to manufacturer's instructions.

## Confocal Microscopy

CHO-K1 or CHO-R7BP cells were plated to achieve a density of  $1 \times 10^5$  cells on 22 mm glass coverslips placed into a 6 well plate. For transient transfection,  $1 \mu\text{g}$  of total plasmid DNA was used per well, and the RGS7:G $\beta_5$  DNA ratio was maintained at 5:1 for both wild-type and mutant RGS7 and G $\beta_5$  constructs. 24 hours after transfection, cells were fixed in 4% paraformaldehyde in PBS for 10 minutes at room temperature, washed twice with PBS and incubated in blocking solution (1% BSA and 0.1% Triton-X 100 in PBS) for 20 minutes. This was followed by a 1 h incubation with anti-GFP antibody diluted in blocking solution. CHO-R7BP cells were incubated with anti-flag antibody for an additional hour for detection of the tagged R7BP. Fluorescein and Cy3 secondary antibodies were diluted in the blocking solution and used for the detection of the green and red fluorescence, respectively. After staining, the coverslips were then rinsed thoroughly in PBS and water, then mounted on glass slides using Antifade reagent containing Dapi (Invitrogen) and imaged using a Leica TCS SP5 laser scanning confocal microscope. Images shown represent a single optical plane selected from at least 10 stacks that were taken for each cell.

## Protein structure modeling

The three-dimensional model of RGS7 was obtained as a homology (comparative) protein structure with SWISS-MODEL and Swiss PdbViewer/Deep View 3.7 (SP5) (41,42) using G $\beta_5$ -RGS9 [Protein Data Bank accession code: 2PBI] (22) as the template. The alignment between bovine RGS7 and residues 1–422 of the mouse RGS9 (22) exhibited 36% identity. The first 42 amino acids in the RGS7 model were automatically omitted by the software during the homology fitting procedure to obtain a “best fit” model. Images, including three dimensional ribbon diagrams were generated using Discovery Studio Visualizer 1.7 (Accelrys, Inc., San Diego, CA, USA).

## RESULTS

Our previous studies showed that the DEP domain of RGS7 was responsible for the inhibition of muscarinic M3 receptor signaling, and that the interaction between the DEP domain and the receptor was blocked by the G $\beta_5$  subunit (30). These data led us to hypothesize that the DEP domain can inhibit the M3R once it dynamically dissociates from G $\beta_5$ . The main goal of the present study was to test this model by disrupting the DEP:G $\beta_5$  interaction via site-directed mutagenesis and characterization of the interaction of the resulting “open” mutants with the M3R.

### Mutational analysis of the interface between the DEP domain of RGS7 and G $\beta_5$

Before the G $\beta_5$ -RGS9 crystal structure became available (22), we attempted to locate the residues essential for the G $\beta_5$ :DEP interaction through amino acid sequence analysis of different DEP domains and G $\beta$  subunits. We searched for the differences between RGS7, which bound to G $\beta_5$  in our pull-down assay, and RGS9, which did not (21), also taking in consideration the NMR structure of the DEP domain of pleckstrin (43). Since both G $\beta_5$  and G $\beta_1$  bound to the DEP domain of RGS7 we also screened for positively charged conserved residues in G $\beta$  subunits. We identified a double mutation (E73S/D74G, abbreviated as ED/SG) in the DEP domain of RGS7, which diminished its binding to G $\beta_5$  (21). Other tested mutations (K54A, R56A/R57A, K60A and H62A in G $\beta_5$  and D29A/R33D/K38S and K52S in RGS7) had no effect on the G $\beta_5$ :DEP interaction (data not shown).

The recently determined crystal structure of the G $\beta_5$ -RGS9 dimer (22) allowed us to generate a three-dimensional homology model of the G $\beta_5$ -RGS7 complex. As expected, the backbones of RGS7 and RGS9 superimposed very well. Like in the G $\beta_5$ -RGS9 complex, in our model, the G $\beta_5$  chain interfaces extensively with the GGL domain of RGS7, and the

Gβ<sub>5</sub>/GGL moiety is sandwiched between the RGS and DEP domains (Fig 1A). We made the assumption that RGS7 and Gβ<sub>5</sub> residues located within 1.5 Å from each other could contribute to the interaction between the two proteins. Amino acid residues F49, L50, F57, F107 and F110 of the RGS7 DEP domain and W107, D259, I282, I283 and F284 of Gβ<sub>5</sub> fit this criterion (Fig. 1B). We substituted these amino acids for alanines, then expressed and characterized the resulting mutants *in vitro* (Figures 2–4).

To study the interaction between RGS7 DEP and Gβ<sub>5</sub> (Fig. 2), we used our previously developed pull-down assay (21,30). The mutants of the DEP domain were expressed as GST fusions in *E.coli*, and the Gβ<sub>5</sub> mutants were expressed in CHO-K1 cells together with the DEP-less C-terminal portion of RGS7 (RGS7<sup>249-469</sup>). Our data show that the double mutation F107A/F110A in the DEP domain leads to a clear reduction of its interaction with Gβ<sub>5</sub>. As shown in Figure 2A, more than 50% of Gβ<sub>5</sub>-RGS7<sup>249-469</sup> complex is bound to the beads containing wild-type GST-DEP, whereas the beads with F107A/F110A mutant GST-DEP could retain only about 12% of the Gβ<sub>5</sub> complex. Other mutations of the DEP domain, F49A/L50A and F57A, did not influence the interaction with Gβ<sub>5</sub>. In Gβ<sub>5</sub>, substitutions of F284 for alanine and the double mutation I282A/I283A also lead to an approximately five-fold reduction in its ability to bind to the RGS7 DEP domain (Figure 2B). The W107A mutation reduced the Gβ<sub>5</sub>:DEP interaction approximately 2-fold, whereas the D259A mutation in Gβ<sub>5</sub> slightly (~10%) increased the fraction of the Gβ<sub>5</sub>-RGS7<sup>249-469</sup> complex absorbed onto the beads with immobilized wild type GST-DEP domain. We also tested association of the Gβ<sub>5</sub> F284A mutant with the F107A/F110A mutant of GST-DEP and found that the simultaneous mutation of both partners diminished their interaction to the level of non-specific binding (Figure 2B).

The diagram presented in Figure 2C summarizes all our data on the mutational analysis of the Gβ<sub>5</sub>:DEP interaction. In our previous study, we identified residues E73 and D74 of RGS7 to be important for association of the DEP domain of RGS7 with the Gβ<sub>5</sub> moiety (21). We have now found that residues F107 and F110 of the DEP domain and three adjacent hydrophobic residues of Gβ<sub>5</sub>, I282, I283 and F284, also contribute to the interaction.

### The role of Gβ<sub>5</sub>:DEP association in the interaction of Gβ<sub>5</sub>-RGS7 with the M3R

Our previous studies suggested that Gβ<sub>5</sub>-RGS7 binds to the receptor only when it is in its open conformation, *i.e.*, when Gβ<sub>5</sub> does not sequester the DEP domain (30). This idea implied that mutations destabilizing the Gβ<sub>5</sub>:DEP interaction should facilitate the transition of the Gβ<sub>5</sub>-RGS7 dimer toward its open conformation, thereby promoting its interaction with the receptor.

We introduced the F107A/F110A double mutation into the full-length RGS7 cDNA, co-expressed this construct with Gβ<sub>5</sub> in CHO-K1 cells and tested it in the pull-down assay with the GST fusion of the 3<sup>rd</sup> intracellular loop of the M3R (Figure 3). In contrast to the dimer composed of wild-type RGS7 and Gβ<sub>5</sub>, this mutant could readily bind to the immobilized M3Ri3. Gβ<sub>5</sub> mutants F284A and the I282A/I283A, when combined with the wild-type RGS7, could not bind to the M3Ri3 loop. However, the Gβ<sub>5</sub> mutations I282A/I283A and particularly F284A augmented the effect of the F107A/F110A mutation of the RGS7. These results corroborate the involvement of residues F107 and F110 of the DEP domain and I282, I283 and F284 of Gβ<sub>5</sub> in the DEP:Gβ<sub>5</sub> interaction (Figures 1, 2). More importantly, they are consistent with the idea that transition of the Gβ<sub>5</sub>-RGS7 dimer to its open conformation facilitates its interaction with the M3R.

In a parallel series of experiments, we tested whether the mutants displaying increased binding to the M3Ri3 loop (*i.e.*, “open” mutants) were also more effective as inhibitors of

M3R-signaling. Figure 4A shows the effect of the different open mutants of G $\beta$ <sub>5</sub>-RGS7 complex on M3R-mediated Ca<sup>2+</sup> mobilization elicited by 100  $\mu$ M carbachol. Contrary to our expectations, the extent of the inhibition conferred by the open mutants was similar to that of the wild-type G $\beta$ <sub>5</sub>-RGS7 dimer. Recently, we showed that G $\beta$ <sub>5</sub>-RGS7 could reduce the amplitude of the Ca<sup>2+</sup> response to M3R stimulation by up to 90% if carbachol concentration was below its K<sub>d</sub> (30). Under such conditions the amplitude of the Ca<sup>2+</sup> response is about four times lower compared to the response at 100  $\mu$ M carbachol, which reduces the overall signal-to-noise ratio, but the inhibitory effect of G $\beta$ <sub>5</sub>-RGS7 on M3R signaling has a wider dynamic range. We tested the open mutants at 1  $\mu$ M carbachol, but did not detect a difference between the effect of wild type and mutant G $\beta$ <sub>5</sub>-RGS7 complexes (data not shown). Our earlier study showed that R7BP precluded wild-type G $\beta$ <sub>5</sub>-RGS7 from inhibiting M3R signaling, whereas the ED/SG mutant was able to inhibit M3R even in the presence of R7BP (21). Therefore, we expected that the G $\beta$ <sub>5</sub>:DEP interface mutations identified in this study could also overcome the effect of R7BP and tested the function of the new open mutants in the presence of R7BP. To limit the number of transfected cDNAs to three (M3R, G $\beta$ <sub>5</sub> and RGS7), we used the previously constructed CHO cell line that stably expresses Flag-tagged R7BP (21). Like the wild-type G $\beta$ <sub>5</sub>-RGS7, the open mutants localized to the plasma membranes in the cells (Figure 4B), indicating that these mutations did not diminish the ability of the RGS7 complex to bind to R7BP. We found that in contrast to the ED/SG mutant, the complexes composed of RGS7 F107A/F110A and G $\beta$ <sub>5</sub> I282A/I283A or F284A mutants behaved similarly to the wild-type G $\beta$ <sub>5</sub>-RGS7 both in the absence and in the presence of R7BP.

Thus, whereas the pull-down assay with the M3Ri3 loop revealed a clear difference between the open mutants identified in this study and wild-type G $\beta$ <sub>5</sub>-RGS7 (Figure 3), the signaling assay with the full-length receptor did not (Figure 4). To explain the apparent discrepancy between the two experiments, we reasoned that the signaling assay involved an additional factor that was absent in the pull-down experiment. The role of this hypothetical factor would be to facilitate the shift of G $\beta$ <sub>5</sub>-RGS7 to its open conformation, so that the wild-type dimer becomes as effective in interacting with the receptor as its “open” mutants. We proposed that such a factor was a region of M3R, which is present in the full-length receptor but is absent in the 3<sup>rd</sup> loop.

### The C-terminus of the M3R plays a role in the interaction with G $\beta$ <sub>5</sub>-RGS7

Since the first and second loops of the M3R are short, we expected the C-tail of the receptor to be a more likely candidate region for the interaction with G $\beta$ <sub>5</sub>-RGS7. To test this hypothesis, we used two complementary approaches. In one series of experiments (Figure 5), we measured Ca<sup>2+</sup> responses elicited by the M3R receptor that lacks a portion of its C-terminus (M3R- $\Delta$ C). This M3R mutant is truncated by a stop codon at position 565, immediately after the putative helix 8, and was earlier shown to retain the ability to signal via phospholipase C and activate MAP kinases (40). In a complimentary approach, we tested whether G $\beta$ <sub>5</sub>-RGS7 could directly interact with the GST fusion of the M3R C-terminus (M3R-C) (Figure 6).

G $\beta$ <sub>5</sub>-RGS7 only marginally reduced the amplitude of the M3R- $\Delta$ C-mediated Ca<sup>2+</sup> response to carbachol, showing that the C-tail is required for G $\beta$ <sub>5</sub>-RGS7 to inhibit M3R signaling (Figure 5A, C). However, we found that the open mutant of G $\beta$ <sub>5</sub>-RGS7 (G $\beta$ <sub>5</sub> F284A plus RGS7 F107A/F110A) could inhibit signaling by the truncated receptor (Figure 5B, C). These results indicate that the C-tail is required for inhibition of the M3R by G $\beta$ <sub>5</sub>-RGS7 and potentially can facilitate the transition of the wild-type G $\beta$ <sub>5</sub>-RGS7 dimer to its open conformation.

The M3R-C GST fusion, which included the entire C-tail, did not bind to the wild-type G $\beta_5$ -RGS7 dimer, but readily bound to the open mutant (Figure 6A). We then asked whether the M3R-C construct could bind to the DEP domain or to G $\beta_5$ , and found that, somewhat surprisingly, that it could bind to both these entities. Whereas the DEP domain bound to the C-termini of M1, M3 and M5 muscarinic receptors equally well (Figure 6B), monomeric G $\beta_5$  or its complex with the DEP-less R7<sup>249-469</sup> construct bound selectively to the C-terminus of the M3R (Figure 6C).

These results indicate that G $\beta_5$ -RGS7 binds to the M3R via both the 3rd intracellular loop and the C-terminal tail.

## DISCUSSION

It is now well appreciated that in addition to G proteins, GPCRs interact with a plethora of partners collectively known as GPCR-interacting proteins (GIPs) (44,45). These diverse proteins modulate G protein signaling and mediate novel pathways that sometimes even bypass the G proteins. Recently, we reported that the muscarinic acetylcholine receptor M3 can directly bind to the regulator of G protein signaling complex, G $\beta_5$ -RGS7, and that this interaction occurs between the DEP domain of RGS7 and the 3<sup>rd</sup> intracellular loop of the M3R (30). In the current paper we focused on further investigating the molecular details of this interaction.

The complexes of the R7 family RGS proteins with G $\beta_5$  were discovered more than a decade ago (15,17), but the significance of their multi-domain organization and, above all, the reason why they integrate the G $\beta\gamma$ -like entity, remained unclear. It was shown that G $\beta_5$  increases the stability of the associated RGS subunit (28,46), and that the DEP domains play a role in plasma membrane targeting via R7BP (18,19). However, stability and membrane anchoring can be achieved via other mechanisms; some RGS proteins function while consisting of little more than the RGS box. A hypothesis explaining the significance of G $\beta_5$ -R7 structural organization began to emerge from the finding that the G $\beta_5$  moiety interacts with the DEP domain, and, particularly, from the evidence of the dynamic nature of this interaction (21). In this model, the dynamic interaction of G $\beta_5$  with the DEP domain enables a functional cycle analogous to the G $\alpha\beta\gamma \rightleftharpoons G\alpha + G\beta\gamma$  cycle of heterotrimeric G proteins. As the G $\beta_5$ -R7 dimer alternates between the distinct “closed” and “open” conformations, it can interact with different binding partners. In the current paper, we developed this idea further by stabilizing the putative open conformation by introducing mutations that impair the interaction between G $\beta_5$  and the DEP domain.

The first step in our study was to identify the amino acids responsible for the DEP:G $\beta_5$  interaction. On the basis of the homology with the tertiary structure of the G $\beta_5$ -RGS9 complex we identified two phenylalanines (F107 and F110) in the DEP domain of RGS7 and the Ile-Ile-Phe triad in G $\beta_5$ , as being important for the interaction (Figures 1–2). These amino acids appear to cause the DEP:G $\beta_5$  association through hydrophobic forces. However, other residues may also contribute to this interaction (Figure 2), and, as we previously showed, substitution of E73 and D74 in RGS7 for the corresponding Ser and Gly residues of RGS9 (ED/SG mutation) also diminished DEP:G $\beta_5$  binding (21). The E73 and D74 residues do not localize at the putative DEP:G $\beta_5$  interface (Fig 1B), making it difficult to explain the phenotype. It is possible that our model of RGS7 is not entirely correct, and that the E73 and D74 residues do, in fact, contact the G $\beta_5$  chain. The sequence identity between our template (murine RGS9 crystal structure) and target (bovine RGS7) is only 36%, which might be too low for reliable homology modeling. Therefore, the structure of RGS7, especially in solution, can deviate from RGS9 far more than that afforded by the best match algorithm. An alternative explanation is that the ED/SG mutation allosterically



influences the position of F107 and F110 at the interface with G $\beta$ <sub>5</sub>. The ED/SG mutation and the mutations at the DEP:G $\beta$ <sub>5</sub> hydrophobic interface result in a clearly distinct phenotype when tested in the presence of R7BP (Figure 4). Consistent with our previous report, the ED/SG mutation was able to overcome the negative effect of R7BP on the ability of G $\beta$ <sub>5</sub>-RGS7 to inhibit M3R signaling. In contrast, open mutants identified in this paper were ineffective in inhibiting M3R signaling in the presence of R7BP (Figure 4A). At the same time, all the mutant forms were capable of binding to R7BP, as was indicated by their ability to localize to the plasma membranes in the R7BP-expressing cells (Figure 4B,C). At the moment, the phenotypic difference between the ED/SG mutant and the new mutations identified in this study is difficult to explain, and we can only speculate that the ED/SG mutation is more effective in promoting the open conformation.

The idea brought about by our structure-function analysis is that, regardless of how specific mutations impair the DEP:G $\beta$ <sub>5</sub> association, they enhance the interaction of the G $\beta$ <sub>5</sub>-RGS7 dimer with the M3R. The ED/SG mutation led to a gain of function in terms of inhibition of M3R signaling in the presence of R7BP (21) (Figure 4A). Similarly, mutations of the hydrophobic DEP:G $\beta$ <sub>5</sub> interface enabled binding of G $\beta$ <sub>5</sub>-RGS7 to the 3<sup>rd</sup> intracellular loop (Figure 3) and the C-tail of the M3R (Figure 6) as well as resulted in the inhibition of the truncated M3R (Figure 5).

In our previous study we identified the 3<sup>rd</sup> intracellular loop of the M3R as the region responsible for the interaction with G $\beta$ <sub>5</sub>-RGS7 (30). We found that deletion of this loop rendered the M3R insensitive to G $\beta$ <sub>5</sub>-RGS7, while recombinant M3Ri3 could directly bind to the isolated DEP domain or the RGS7 monomer. Interestingly, the full-length G $\beta$ <sub>5</sub>-RGS7 dimer could not bind to the M3Ri3 *in vitro*, which made it difficult to explain how the dimer could inhibit M3R signaling. We hypothesized that G $\beta$ <sub>5</sub>-RGS7 can bind to the M3R after assuming the open conformation, the notion supported in this paper (Figures 3, 6A). We also reasoned that mutations that facilitate binding of G $\beta$ <sub>5</sub>-RGS7 to M3Ri3 should increase the apparent effectiveness of G $\beta$ <sub>5</sub>-RGS7 as an inhibitor of M3R signaling. However, our assays did not detect such an enhanced activity (Figure 4).

To explain the similarity between the wild-type and mutant G $\beta$ <sub>5</sub>-RGS7 in their ability to inhibit M3R signaling, we extended our model. We postulated that the receptor has an intrinsic capacity to *induce* the open conformation in G $\beta$ <sub>5</sub>-RGS7 and that this capability is associated with an M3R region that is distinct from the third loop. This prediction proved to be correct: we found that the C-tail of the receptor can interact with G $\beta$ <sub>5</sub>-RGS7 (Figures 5, 6). Truncation of the C-terminus rendered the M3R insensitive to the inhibition by the wild-type G $\beta$ <sub>5</sub>-RGS7, but interestingly, the open G $\beta$ <sub>5</sub>-RGS7 mutant could inhibit the truncated receptor (Figure 5). In other words, the G $\beta$ <sub>5</sub>-RGS7 molecule that has already been opened by a mutation does not require the M3R C-tail to do so.

Our data show that the isolated C-tail cannot bind to the wild-type G $\beta$ <sub>5</sub>-RGS7 but does bind the open mutant, which implies synergy between the C-tail and the 3<sup>rd</sup> intracellular loop in the process of G $\beta$ <sub>5</sub>-RGS7 recruitment. G $\beta$ <sub>5</sub> binds to the C-tail of M3R in a selective manner, indicating that it associates with the sequence unique for the M3 subtype. The C-tail of the M3R can now be added to the list of putative binding partners of G $\beta$ <sub>5</sub>, in addition to G $\alpha$ i and PLC, which in early studies were shown to interact with G $\beta$ <sub>5</sub> $\gamma$  (47–50). On the other hand, the DEP domain of RGS7 appears to bind to both the C-tail and M3Ri3. A more detailed structure-function analysis will be needed to further dissect molecular events involved in the interaction of M3R with G $\beta$ <sub>5</sub>-RGS7. Since M3R can oligomerize (51), it is possible that G $\beta$ <sub>5</sub>-RGS7, being a rather large molecule, can simultaneously bind to the C-tail of one M3R molecule and the 3<sup>rd</sup> loop of another.

Interaction of M3R with G $\beta_5$ -RGS7 supports the emerging concept that GPCRs can form complexes with RGS proteins (52–56). For example, yeast RGS protein Sst2 that is unrelated to the R7 family can directly bind to the GPCR Ste2 (57). That study is particularly interesting in relation to the current paper because the Ste2:Sst2 interaction requires the C-tail of the Ste2 receptor and the DEP domain present in Sst2. The results of another group indicated that RGS9 also associated via its DEP domain with the dopamine D2 receptor (58). Our current paper extends our understanding of the role of the DEP and G $\beta_5$ /GGL entities in the R7 family by showing that their dissociation in the G $\beta_5$ -RGS7 complex can facilitate its interaction with the M3R. The identification of the M3R C-terminus as the site essential for in the interaction with G $\beta_5$ -RGS7 provides an additional mechanistic insight into the interaction between this receptor and the G $\beta_5$ -RGS7 complex.

## Acknowledgments

Supported by NIH grant GM 060019 (V.Z.S.)

We thank Dr. Andrew Tobin (University of Leicester) for DNA constructs.

## Abbreviations are

<b>RGS</b>	regulator of G protein signaling
<b>R7BP</b>	R7 family RGS protein binding protein
<b>GPCR</b>	G protein-coupled receptor
<b>GST</b>	glutathione-S-transferase
<b>CFP and YFP</b>	cyan and yellow versions of green fluorescent protein (GFP)
<b>CHO</b>	Chinese hamster ovary

## References

1. Limbird LE, Gill DM, Lefkowitz RJ. Agonist-promoted coupling of the beta-adrenergic receptor with the guanine nucleotide regulatory protein of the adenylate cyclase system. *Proc Natl Acad Sci U S A*. 1980; 77:775–779. [PubMed: 6244585]
2. Fung BK, Hurley JB, Stryer L. Flow of information in the light-triggered cyclic nucleotide cascade of vision. *Proc Natl Acad Sci U S A*. 1981; 78:152–156. [PubMed: 6264430]
3. Northup JK, Smigel MD, Sternweis PC, Gilman AG. The subunits of the stimulatory regulatory component of adenylate cyclase. Resolution of the activated 45,000-dalton (alpha) subunit. *J Biol Chem*. 1983; 258:11369–11376. [PubMed: 6309844]
4. Clapham DE, Neer EJ. New roles for G-protein beta gamma-dimers in transmembrane signalling. *Nature*. 1993; 365:403–406. [PubMed: 8413584]
5. Neer EJ, Clapham DE. Roles of G protein subunits in transmembrane signalling. *Nature*. 1988; 333:129–134. [PubMed: 3130578]
6. Smrcka AV. G protein betagamma subunits: central mediators of G protein-coupled receptor signaling. *Cell Mol Life Sci*. 2008; 65:2191–2214. [PubMed: 18488142]
7. Dohlman HG, Thorner J. RGS proteins and signaling by heterotrimeric G proteins. *J Biol Chem*. 1997; 272:3871–3874. [PubMed: 9064301]
8. Berman DM, Gilman AG. Mammalian RGS proteins: barbarians at the gate. *J Biol Chem*. 1998; 273:1269–1272. [PubMed: 9430654]
9. Hepler JR. Emerging roles for RGS proteins in cell signalling. *Trends Pharmacol Sci*. 1999; 20:376–382. [PubMed: 10462761]
10. Chidiac P, Roy AA. Activity, regulation, and intracellular localization of RGS proteins. *Receptors Channels*. 2003; 9:135–147. [PubMed: 12775336]

11. Willars GB. Mammalian RGS proteins: multifunctional regulators of cellular signalling. *Semin Cell Dev Biol.* 2006; 17:363–376. [PubMed: 16687250]
12. Witherow DS, Slepak VZ. A Novel Kind of G Protein Heterodimer: The Gbeta5-RGS Complex. *Receptors Channels.* 2003; 9:205–212. [PubMed: 12775340]
13. Anderson GR, Posokhova E, Martemyanov KA. The R7 RGS protein family: multi-subunit regulators of neuronal G protein signaling. *Cell Biochem Biophys.* 2009; 54:33–46. [PubMed: 19521673]
14. Slepak, VZ. Structure, Function, and Localization of Gbeta5-RGS Complexes. In: Fisher, Rory A., editor. *Progress in Molecular Biology and Translational Science.* Vol. 86. Academic Press; 2009. p. 157-203.
15. Cabrera JL, de Freitas F, Satpaev DK, Slepak VZ. Identification of the Gbeta5-RGS7 protein complex in the retina. *Biochem Biophys Res Commun.* 1998; 249:898–902. [PubMed: 9731233]
16. Levay K, Cabrera JL, Satpaev DK, Slepak VZ. Gbeta5 prevents the RGS7-Galphao interaction through binding to a distinct Ggamma-like domain found in RGS7 and other RGS proteins. *Proc Natl Acad Sci U S A.* 1999; 96:2503–2507. [PubMed: 10051672]
17. Snow BE, Krumins AM, Brothers GM, Lee SF, Wall MA, Chung S, Mangion J, Arya S, Gilman AG, Siderovski DP. A G protein gamma subunit-like domain shared between RGS11 and other RGS proteins specifies binding to Gbeta5 subunits. *Proc Natl Acad Sci U S A.* 1998; 95:13307–13312. [PubMed: 9789084]
18. Drenan RM, Doupnik CA, Boyle MP, Muglia LJ, Huettner JE, Linder ME, Blumer KJ. Palmitoylation regulates plasma membrane-nuclear shuttling of R7BP, a novel membrane anchor for the RGS7 family. *J Cell Biol.* 2005; 169:623–633. [PubMed: 15897264]
19. Martemyanov KA, Yoo PJ, Skiba NP, Arshavsky VY. R7BP, a novel neuronal protein interacting with RGS proteins of the R7 family. *J Biol Chem.* 2005; 280:5133–5136. [PubMed: 15632198]
20. Jayaraman M, Zhou H, Jia L, Cain MD, Blumer KJ. R9AP and R7BP: traffic cops for the RGS7 family in phototransduction and neuronal GPCR signaling. *Trends Pharmacol Sci.* 2008
21. Narayanan V, Sandiford SL, Wang Q, Keren-Raifman T, Levay K, Slepak VZ. Intramolecular Interaction between the DEP Domain of RGS7 and the Gbeta(5) Subunit. *Biochemistry.* 2007; 46:6859–6870. [PubMed: 17511476]
22. Cheever ML, Snyder JT, Gershburg S, Siderovski DP, Harden TK, Sondek J. Crystal structure of the multifunctional Gbeta5-RGS9 complex. *Nat Struct Mol Biol.* 2008; 15:155–162. [PubMed: 18204463]
23. Hooks SB, Martemyanov K, Zachariou V. A role of RGS proteins in drug addiction. *Biochem Pharmacol.* 2008; 75:76–84. [PubMed: 17880927]
24. Hooks SB, Waldo GL, Corbitt J, Bodor ET, Krumins AM, Harden TK. RGS6, RGS7, RGS9, and RGS11 stimulate GTPase activity of Gi family G-proteins with differential selectivity and maximal activity. *J Biol Chem.* 2003; 278:10087–10093. [PubMed: 12531899]
25. Hajdu-Cronin YM, Chen WJ, Patikoglou G, Koelle MR, Sternberg PW. Antagonism between G(o)alpha and G(q)alpha in *Caenorhabditis elegans*: the RGS protein EAT-16 is necessary for G(o)alpha signaling and regulates G(q)alpha activity. *Genes Dev.* 1999; 13:1780–1793. [PubMed: 10421631]
26. Chase DL, Patikoglou GA, Koelle MR. Two RGS proteins that inhibit Galpha(o) and Galpha(q) signaling in *C. elegans* neurons require a Gbeta(5)-like subunit for function. *Curr Biol.* 2001; 11:222–231. [PubMed: 11250150]
27. Patikoglou GA, Koelle MR. An N-terminal region of *Caenorhabditis elegans* RGS proteins EGL-10 and EAT-16 directs inhibition of G(alpha)o versus G(alpha)q signaling. *J Biol Chem.* 2002; 277:47004–47013. [PubMed: 12354761]
28. Witherow DS, Wang Q, Levay K, Cabrera JL, Chen J, Willars GB, Slepak VZ. Complexes of the G protein subunit gbeta 5 with the regulators of G protein signaling RGS7 and RGS9. Characterization in native tissues and in transfected cells. *J Biol Chem.* 2000; 275:24872–24880. [PubMed: 10840031]
29. Witherow DS, Tovey SC, Wang Q, Willars GB, Slepak VZ. G beta 5. RGS7 inhibits G alpha q-mediated signaling via a direct protein-protein interaction. *J Biol Chem.* 2003; 278:21307–21313. [PubMed: 12670932]

30. Sandiford S, Slepak V. G $\beta$ 5-RGS7 selectively inhibits muscarinic M3 receptor signaling via the interaction between the third intracellular loop of the receptor and the DEP domain of RGS7. *Biochemistry*. 2009; 48:2282–2289. [PubMed: 19182865]
31. Wess J, Brann MR, Bonner TI. Identification of a small intracellular region of the muscarinic m3 receptor as a determinant of selective coupling to PI turnover. *FEBS Lett*. 1989; 258:133–136. [PubMed: 2556294]
32. Wu G, Krupnick JG, Benovic JL, Lanier SM. Interaction of arrestins with intracellular domains of muscarinic and alpha2-adrenergic receptors. *J Biol Chem*. 1997; 272:17836–17842. [PubMed: 9211939]
33. Wu G, Benovic JL, Hildebrandt JD, Lanier SM. Receptor docking sites for G-protein betagamma subunits. Implications for signal regulation. *J Biol Chem*. 1998; 273:7197–7200. [PubMed: 9516410]
34. Wu G, Bogatkevich GS, Mukhin YV, Benovic JL, Hildebrandt JD, Lanier SM. Identification of Gbetagamma binding sites in the third intracellular loop of the M(3)-muscarinic receptor and their role in receptor regulation. *J Biol Chem*. 2000; 275:9026–9034. [PubMed: 10722752]
35. Lucas JL, Wang D, Sadee W. Calmodulin binding to peptides derived from the i3 loop of muscarinic receptors. *Pharm Res*. 2006; 23:647–653. [PubMed: 16552497]
36. Simon V, Guidry J, Gettys TW, Tobin AB, Lanier SM. The proto-oncogene SET interacts with muscarinic receptors and attenuates receptor signaling. *J Biol Chem*. 2006; 281:40310–40320. [PubMed: 17065150]
37. Budd DC, McDonald JE, Tobin AB. Phosphorylation and regulation of a Gq/11-coupled receptor by casein kinase 1alpha. *J Biol Chem*. 2000; 275:19667–19675. [PubMed: 10777483]
38. Luo J, Busillo JM, Benovic JL. M3 muscarinic acetylcholine receptor-mediated signaling is regulated by distinct mechanisms. *Mol Pharmacol*. 2008; 74:338–347. [PubMed: 18388243]
39. Witherow DS, Slepak VZ. Biochemical purification and functional analysis of complexes between the G-protein subunit Gbeta5 and RGS proteins. *Methods Enzymol*. 2004; 390:149–162. [PubMed: 15488176]
40. Budd DC, McDonald J, Emsley N, Cain K, Tobin AB. The C-terminal tail of the M3-muscarinic receptor possesses anti-apoptotic properties. *J Biol Chem*. 2003; 278:19565–19573. [PubMed: 12649280]
41. Guex N, Peitsch MC. SWISS-MODEL and the Swiss-PdbViewer: an environment for comparative protein modeling. *Electrophoresis*. 1997; 18:2714–2723. [PubMed: 9504803]
42. Guex N, Peitsch MC, Schwede T. Automated comparative protein structure modeling with SWISS-MODEL and Swiss-PdbViewer: a historical perspective. *Electrophoresis*. 2009; 30(Suppl 1):S162–173. [PubMed: 19517507]
43. Civera C, Simon B, Stier G, Sattler M, Macias MJ. Structure and dynamics of the human pleckstrin DEP domain: distinct molecular features of a novel DEP domain subfamily. *Proteins*. 2005; 58:354–366. [PubMed: 15573383]
44. Brady AE, Limbird LE. G protein-coupled receptor interacting proteins: emerging roles in localization and signal transduction. *Cell Signal*. 2002; 14:297–309. [PubMed: 11858937]
45. Bockaert J, Fagni L, Dumuis A, Marin P. GPCR interacting proteins (GIP). *Pharmacol Ther*. 2004; 103:203–221. [PubMed: 15464590]
46. Chen CK, Eversole-Cire P, Zhang H, Mancino V, Chen YJ, He W, Wensel TG, Simon MI. Instability of GGL domain-containing RGS proteins in mice lacking the G protein beta-subunit Gbeta5. *Proc Natl Acad Sci U S A*. 2003; 100:6604–6609. [PubMed: 12738888]
47. Watson AJ, Katz A, Simon MI. A fifth member of the mammalian G-protein beta-subunit family. Expression in brain and activation of the beta 2 isotype of phospholipase C. *J Biol Chem*. 1994; 269:22150–22156. [PubMed: 8071339]
48. Watson AJ, Aragay AM, Slepak VZ, Simon MI. A novel form of the G protein beta subunit Gbeta5 is specifically expressed in the vertebrate retina. *J Biol Chem*. 1996; 271:28154–28160. [PubMed: 8910430]
49. Zhang S, Coso OA, Lee C, Gutkind JS, Simonds WF. Selective activation of effector pathways by brain-specific G protein beta5. *J Biol Chem*. 1996; 271:33575–33579. [PubMed: 8969224]

50. Yoshikawa DM, Hatwar M, Smrcka AV. G protein beta 5 subunit interactions with alpha subunits and effectors. *Biochemistry*. 2000; 39:11340–11347. [PubMed: 10985779]
51. Zeng F, Wess J. Molecular aspects of muscarinic receptor dimerization. *Neuropsychopharmacology*. 2000; 23:S19–31. [PubMed: 11008064]
52. Bernstein LS, Ramineni S, Hague C, Cladman W, Chidiac P, Levey AI, Hepler JR. RGS2 binds directly and selectively to the M1 muscarinic acetylcholine receptor third intracellular loop to modulate Gq/11alpha signaling. *J Biol Chem*. 2004; 279:21248–21256. [PubMed: 14976183]
53. Georgoussi Z, Leontiadis L, Mazarakou G, Merkouris M, Hyde K, Hamm H. Selective interactions between G protein subunits and RGS4 with the C-terminal domains of the mu- and delta-opioid receptors regulate opioid receptor signaling. *Cell Signal*. 2006; 18:771–782. [PubMed: 16120478]
54. Schwendt M, McGinty JF. Regulator of G-protein signaling 4 interacts with metabotropic glutamate receptor subtype 5 in rat striatum: relevance to amphetamine behavioral sensitization. *J Pharmacol Exp Ther*. 2007; 323:650–657. [PubMed: 17693584]
55. Langer I, Tikhonova IG, Boulegue C, Esteve JP, Vatinel S, Ferrand A, Moroder L, Robberecht P, Fourmy D. Evidence for a direct and functional interaction between the regulators of G protein signaling-2 and phosphorylated C terminus of cholecystokinin-2 receptor. *Mol Pharmacol*. 2009; 75:502–513. [PubMed: 19064631]
56. Abramow-Newerly M, Roy AA, Nunn C, Chidiac P. RGS proteins have a signalling complex: interactions between RGS proteins and GPCRs, effectors, and auxiliary proteins. *Cell Signal*. 2006; 18:579–591. [PubMed: 16226429]
57. Ballon DR, Flanary PL, Gladue DP, Konopka JB, Dohlman HG, Thorner J. DEP-domain-mediated regulation of GPCR signaling responses. *Cell*. 2006; 126:1079–1093. [PubMed: 16990133]
58. Kovoov A, Seyffarth P, Ebert J, Barghshoon S, Chen CK, Schwarz S, Axelrod JD, Cheyette BN, Simon MI, Lester HA, Schwarz J. D2 dopamine receptors colocalize regulator of G-protein signaling 9-2 (RGS9-2) via the RGS9 DEP domain, and RGS9 knock-out mice develop dyskinesias associated with dopamine pathways. *J Neurosci*. 2005; 25:2157–2165. [PubMed: 15728856]

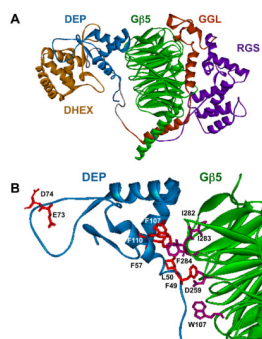


**Figure 1. Molecular model of the G $\beta$ <sub>5</sub>-RGS7 dimer**

(A) Ribbon diagram presentation of the homology model of the G $\beta$ <sub>5</sub>-RGS7 complex constructed on the basis of PDB coordinates of the crystal structure of the G $\beta$ <sub>5</sub>-RGS9-1 complex (22). The G $\beta$ <sub>5</sub> polypeptide chain is shown in green. The domains of RGS7 are highlighted in the following colors: DEP, blue; DHEX, light brown; GGL, red; RGS, purple. In this projection the doughnut-shaped G $\beta$ <sub>5</sub> structure is seen from the side. G $\beta$ <sub>5</sub> makes multiple contacts with the GGL domain, and the G $\beta$ <sub>5</sub>-GGL complex resides between the DEP and RGS domains. The area of contact between the DEP domain and G $\beta$ <sub>5</sub> is shown in more detail in (B). (B) The DEP:G $\beta$ <sub>5</sub> interface. Amino acids that are found within the 1.5 Å radius from the opposite chain are shown in red (RGS7) and purple (G $\beta$ <sub>5</sub>).

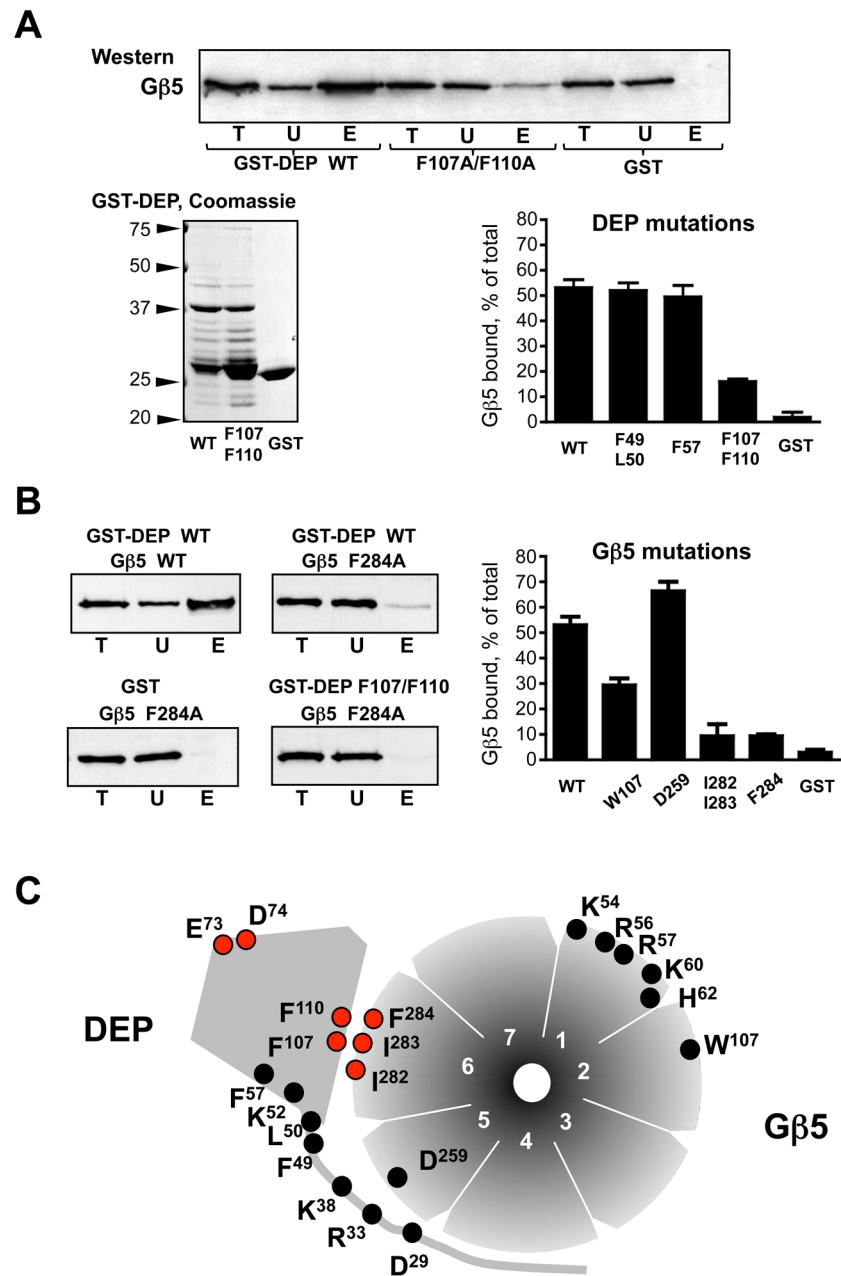


**Figure 2. Mutational analysis of the DEP:Gβ<sub>5</sub> interface**

Indicated amino acids of the RGS7 DEP domain or Gβ<sub>5</sub> were substituted. Residues D29, R33, K38, K52, E73 and D74 were changed to the corresponding RGS9 residues, and all other residues were substituted by alanines, as described in Materials and Methods. (A) Analysis of the RGS7 DEP domain mutants. The DEP domain mutants were expressed as GST fusion proteins and analyzed by SDS-PAGE and Coomassie Blue staining. Along with the full-length GST-DEP fusion protein (~38 kDa) these preparations contained apparent degradation products, which were similar among all the DEP mutants. The wild-type and mutant GST-DEP proteins were immobilized on glutathione beads, so that the amounts of the fusion proteins were equal and corresponded to the amount of GST immobilized on the control beads. The complex of wild-type Gβ<sub>5</sub> with the RGS7<sup>249-469</sup> construct was expressed

in CHO-K1 cells by transient transfection, and the cell lysate was subjected to the GST pull-down, as described in Materials and Methods. The western blot panel shows a representative experiment where the G $\beta$ <sub>5</sub>-RGS7<sup>249-469</sup> complex was tested for binding with the beads containing the GST fusion of wild type DEP domain (WT), the double-mutant F107A/F110A, or GST. The beads were washed and then eluted with SDS-containing sample buffer. The total CHO-K1 cell lysate (T), the unbound (U) and the eluate (E) fractions were probed with the anti-G $\beta$ <sub>5</sub> antibody, followed by ECL detection. The films were scanned and analyzed with Scion software. The bar graph summarizes the quantification of the data obtained from the entire series of experiments with all tested RGS7 DEP mutants. Material in the eluate (E) fractions was 5 times more concentrated relative to the unbound or total to ensure that the resulting ECL signal was within the linear range of detection. The values of the amount of G $\beta$ <sub>5</sub> present in the analyzed fractions was calculated accordingly and presented as the percentage of G $\beta$ <sub>5</sub> eluted from the beads relative to the total amount of G $\beta$ <sub>5</sub> in the cell lysate. Shown are the mean values with error bars representing standard deviation from 3–6 independent experiments. (B) Analysis of G $\beta$ <sub>5</sub> mutations. The indicated G $\beta$ <sub>5</sub> mutants were expressed in CHO cells in a complex with the RGS7<sup>249-469</sup> construct and tested for their ability to bind to wild-type GST-DEP using the pull-down described in (A). Representative western blots show the total lysate (T) unbound (U) and eluted (E) fractions analyzed by immunoblot using the antibodies against G $\beta$ <sub>5</sub>. The lower right panel shows the experiment where the G $\beta$ <sub>5</sub> F284A mutant was tested for binding with the F107A/F110A mutant of GST-DEP. The bar graph depicts quantification of the data from 3–4 independent experiments with four G $\beta$ <sub>5</sub> mutants (W107A, D259A, F284A and the I282A/I283A double-mutant) binding to wild-type GST-DEP or GST. (C) Diagram summarizing our mutational analysis of G $\beta$ <sub>5</sub> and RGS7. The seven blades of the G $\beta$ <sub>5</sub> “ $\beta$ -propeller” are numbered 1 through 7. The indicated mutants were tested in the GST pull-down assays described in A and B; the E73S/D74G mutation was described in our earlier study (21). The mutations resulting in a reduction of DEP-G $\beta$ <sub>5</sub> interaction are denoted by the red circles, those without a distinct phenotype are marked in black.



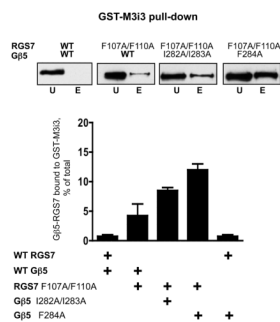


**Figure 3. Interaction of the “open” mutants of Gβ<sub>5</sub>-RGS7 with the third intracellular loop of the M3R**

The GST fusion of the M3Ri3 was immobilized on the glutathione beads. Wild-type or mutant RGS7 constructs were expressed in CHO-K1 cells as full-length proteins fused to the C-terminus of YFP, together with wild-type or mutant Gβ<sub>5</sub>. The cell lysates were subjected to the GST pull-down. Following the incubation with the beads, the unbound and eluted material was analyzed by western blotting using the anti-YFP antibody. The different combinations of WT and mutant constructs used are indicated above the four representative immunoblot panels. The amount of RGS7 bound to the M3i3 beads was determined as the fraction of the total amount of RGS7 in the cell lysate. The total was calculated as the sum of the signal in the unbound and eluted fractions, as described in the Materials and Methods. The data show the mean and standard deviation from three or four independent experiments.

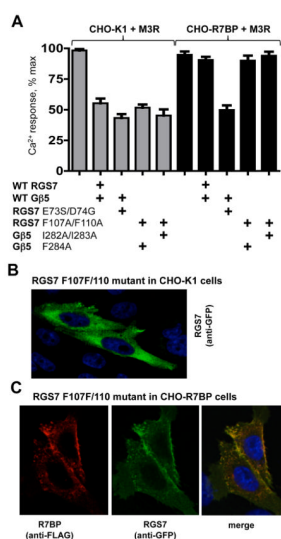


**Figure 4. Effect of open mutations and R7BP on Gβ<sub>5</sub>-RGS7-mediated inhibition of M3R signaling**

(A) The stable cell line expressing flag-tagged R7BP (CHO-R7BP, black bars) was transfected with the M3R together with plasmids encoding the indicated mutants or wild-type Gβ<sub>5</sub> and RGS7. CHO-K1 cells (gray bars) were used as the control lacking R7BP. The transfected cells were analyzed to determine the peak Ca<sup>2+</sup> responses to application of 100 μM carbachol, as described in the Materials and Methods. The data represent the mean ± the standard deviation of the peak Ca<sup>2+</sup> response measured in four independent transfection experiments. (B) CHO-K1 cells were co-transfected with plasmids encoding the F284A mutant of Gβ<sub>5</sub> and the F107A/F110A of RGS7, which was fused to the C-terminus of YFP. The cells were then fixed and stained with anti-GFP antibody (1:5000) as described in Materials and Methods. Blue shows staining with Dapi to localize the cell nuclei. (C) The F284A mutant of Gβ<sub>5</sub> and the F107A/F110A of RGS7 were co-expressed, via transient transfection, in the stable CHO cell line expressing Flag-tagged R7BP. As in (B), the RGS7 mutant was expressed as the YFP fusion protein. The cells were fixed and stained with anti-GFP antibody (1:5000) to detect the localization of the Gβ<sub>5</sub>-RGS7 complex (green) and anti-flag antibody (1:5000) to detect R7BP (red).

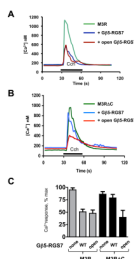


**Figure 5. The C terminus of the M3R is essential for the inhibitory action of Gβ<sub>5</sub>-RGS7 on M3R signaling**

CHO-K1 cells were transiently transfected with M3R, Gβ<sub>5</sub> and RGS7 constructs. Cells were grown on glass coverslips, then loaded with fura-2AM and mounted in a flow chamber at the stage of an inverted fluorescence microscope. Changes in free intracellular Ca<sup>2+</sup> concentrations in response to stimulation with 100 μM carbachol were recorded in real time from the entire field which contained at least 40 cells, as described in Materials and Methods. The application of carbachol (Cch) is denoted with the black bar. (A) Representative traces from cells transfected with plasmids encoding the M3R and Lac Z cDNAs (green), the M3R together with wild-type Gβ<sub>5</sub>-RGS7 (blue) or the M3R with “open” Gβ<sub>5</sub>-RGS7 composed of RGS7 F107A/F110A and Gβ<sub>5</sub> F284A mutants (dark red). (B) The M3R construct lacking its C-terminus (M3RΔC) was co-transfected with the wild-type or the open mutant of Gβ<sub>5</sub>-RGS7. (C). Quantification of the data from four independent experiments showing the mean ± SD of the peak Ca<sup>2+</sup> response expressed as the percent of the maximal detected Ca<sup>2+</sup> response. Gray bars show inhibition of full-length M3R by wild-type Gβ<sub>5</sub>-RGS7 or the open mutant, black bars represent the results with the truncated M3R mutant, M3RΔC.

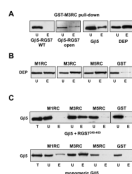


**Figure 6. The C terminus of the M3R directly binds to the DEP domain of RGS7, G $\beta$ <sub>5</sub> and the open mutant of G $\beta$ <sub>5</sub>-RGS7**

(A) The C-terminus of the M3R was expressed in *E.coli* as a GST fusion protein and used to pull down the lysates of CHO cells expressing either the wild-type G $\beta$ <sub>5</sub>-RGS7 dimer, the G $\beta$ <sub>5</sub>-RGS7 dimer composed of the RGS7 F107A/F110A and G $\beta$ <sub>5</sub> F284A mutants (the open mutant), the DEP domain or G $\beta$ <sub>5</sub>. In these experiments, RGS7 and G $\beta$ <sub>5</sub> were fused to YFP and CFP, respectively, and their presence in the unbound (U) and eluted (E) fractions was detected using an anti-GFP antibody. The pull-down was performed as described in Materials and Methods, and similarly to experiments shown in Figures 2 and 3. (B) The C-termini of muscarinic receptors M1, M3 and M5 were expressed as GST fusion proteins and used to pull down the YFP fusion of the DEP domain of RGS7. Beads with GST were used as a negative control. (C) The GST fusions of the C-termini of M1, M3 and M5 muscarinic receptors were used to pull-down the untagged monomeric G $\beta$ <sub>5</sub> or its dimer with the RGS7<sup>249-469</sup> construct. Anti-G $\beta$ <sub>5</sub> antibody was used to probe the unbound and eluted fractions in the assays. Each western blot is a representative of at least three independent experiments.